2021 60th IEEE Conference on Decision and Control (CDC)
December 13-15, 2021. Austin, Texas

Time-Inverted Kuramoto Dynamics for κ-Clustered Circle Coverage

Manuel Boldrer, Francesco Riz, Fabio Pasqualetti, Luigi Palopoli, Daniele Fontanelli

2021 60th IEEE Conference on Decision and Control (CDC) | 978-1-6654-3659-5/21/$31.00 ©2021 IEEE | DOI: 10.1109/CDC45484.2021.9683310

Abstract— **In this paper we analyse the equilibrium configurations for the time-inverted Kuramoto Model with homogeneous agents and a fixed ring topology, where time-inverted means that the coupling between the different states is via a negative factor. This model exhibits a dual behaviour with respect to the classic Kuramoto Model with a positive coupling. In the paper, we show the existence of two possible stable equilibrium configurations: the splay state formation (1-clustered coverage) and the deployment in clusters (κ-clustered coverage). We provide sufficient conditions for the splay state formation and a stability analysis for the networked system. Moreover, we provide some initial results towards the controllability of the final equilibrium configurations. In particular, we lay the foundations to understand the conditions to switch between stable equilibria.**

I. INTRODUCTION

Distributed control of multi-agent systems is a very active research area, both in the control and in the robotics communities. In these fields, one of the topics that received the most attention is the emergence of collective behaviours from the combination of local interaction rules [1], [2]. The Kuramoto Model [3] falls in this class of models.
A Kuramoto model is defined by

$$\dot{\theta}_i = \gamma \sum_{j=0}^{N} a_{ij} \sin(\theta_j - \theta_i).$$

where the varaibles $\theta_1, \theta_2, \ldots, \theta_N$ represent the state of a number of different agents. When $\gamma = +1$, we will say that the states are *positively coupled*, while for $\gamma = -1$ we will say that they are *negatively coupled* (i.e., the system is time-inverted).
Over the years, much of the attention on the Kuramoto model has been on the synchronisation of oscillators. If each state θ_i represents the phase of an oscillator, it can be shown that under some conditions the phases will eventually converge to the same value and the oscillators be synchronised [4] *if* the different states are positively coupled. Much less studied is the case when the oscillators are negatively coupled. One interesting behaviour that emerges in this case is one in which the different states are equally spaced: the so called splay state. The splay state is very much studied in different communities from the neurosciences [5] and to vehicle coordination [6].

M. Boldrer and D. Fontanelli are with the Deparment of Industrial Engineering, University of Trento, Italy {manuel.boldrer, daniele.fontanelli}@unitn.it

F. Riz, L. Palopoli are with the Department of Information Engineering and Computer Science, University of Trento, Italy {francesco.riz, luigi.palopoli}@unitn.it

F. Pasqualetti is with Department of Mechanical Engineering at the University of California, Riverside, fabiopas@engr.ucr.edu

In the robotics community, a coordination scheme that provably and robustly converges to the splay state has profound and far reaching implications. In the wide range of the possibile applications, we can select two paradigmatic examples. As a first example, consider the problem of deploying a number of robots along a closed circular curve that encloses an area of interest. If each robot has a limited sensing range, the splay state is the configuration of the agents that minimises the probability for an intruder to penetrate unnoticed into the area. As a second example, consider a number of robots approaching a shared area (e.g., an intesection). If the states are related to the time each agent is allowed to move, the splay state is the schedule that maximises the time interval between two successive accesses to the shared area.
For all these applications it is imperative to know under which conditions the splay state can be reliably reached and if this evolution can be "forced" through appropiate input actions.

A. Related work

In 1967 Winfree [7] first proposed a coupled oscillator model by considering a general interaction rule among the agents. The Kuramoto Model properly said was first introduced in 1975 [8], giving rise to a research area which has remained active . The large majority of researchers focused on the use of Kuramoto Model for synchronisation purposes. Monzón et al. [9] studied the global stability properties of the Kuramoto Model under the assumption of complete visibility graph between the oscillators. The assumption of complete visibility graph is relaxed in the analysis proposed by Jadbabaie et al. [10]. More recently, hybrid coupling functions have been used in [11] to prove uniform global asymptotic stability, while conditions for cluster synchronisation are studied in [12].
As clearly recognised in the survey of Dörfler et al. [4], the use of positively coupled Kuramoto Model for the phase synchronisation has been studied much more in depth that the use of negatively coupled Kuramoto Model, which is related to the phase balancing problem. Sepulchre et al. provide results on homogeneous agents local phase balancing, in both cases of a mesh [13] or of a general [14] communication framework. Xu et al. in [15] analysed a Kuramoto-like dynamics with sine-terms replaced by cosines to achieve a splay formation (i.e., the agents are deployed uniformly over the circle), however they require a strict condition on the incidence matrix associated to the graph topology. In [16] the authors analyse the interaction between conformist and contrarians oscillators, with positive and negative coupling strength. In [17] the phase balancing problem is studied for

Liénard-type oscillators. Methods to achieve splay state formations for impulse-coupled oscillators are provided in [18], [19], while in [20] Marshall et al. propose a simple control law to achieve circular pursuit patterns, they show that under the proposed control law the equilibrium formations are generalised regular polygons.

B. Paper contributions

In this paper, we restrict our focus to the negatively coupled Kuramoto Model. The main difference with respect to previous works on Kuramoto-based phase balance problem [14] can be found on the chosen communication topology between the agents. We assume to have a time-invariant ring graph topology. Thanks to this choice, we can expose important properties on the dynamic behaviour of the system. Our contributions are threefold: i. we state a sufficient condition for agents to reach splay state configuration; ii. we analyse all the stable configurations of the system that can occur, characterising their degree of stability; iii. we offer a preliminary analysis on how to set up a control scheme that enables to drive the system state from one stable configuration to another.

The paper is organised as follows. In Sec. II we provide a formal description of the problem. In Sec. III we characterise the different equilibrium configurations and analyse their stability. In Sec. IV we offer a preliminary discussion on how to drive the system into a specific equilibrium configuration. Finally, in Sec. V we offer our conclusions and announce future work directions.

II. PROBLEM DESCRIPTION

We consider a set of N agents moving on a circle and following the Kuramoto Model with inverse coupling

$$\dot{\theta}_i = -\sum_{j=0}^{N} a_{ij} \sin(\theta_j - \theta_i) \tag{1}$$

where θ_i denotes the position on the circle of the i–th agent, and $a_{ij} \geq 0$ the coupling between them. In particular, we assume that the agents are coupled according to undirected circulant topology [21], where $A = [a_{ij}]$ with $A \in \mathbb{R}^{N\times N}$ is the following symmetric matrix

$$A = \begin{bmatrix} c_0 & c_1 & \cdots & c_2 & c_1 \\ c_1 & c_0 & c_1 & \cdots & c_2 \\ \vdots & c_1 & c_0 & \ddots & \vdots \\ c_2 & & \ddots & \ddots & c_1 \\ c_1 & c_2 & \cdots & c_1 & c_0 \end{bmatrix}, \tag{2}$$

with $c_0 = 0$ and all the other entries that can be either 0 or 1. Notice that the matrix A corresponds to a generic circulant matrix with the constraint of symmetry, since we are going to consider only undirected graph topologies. In compact form the dynamics of the interconnected agents read as

$$\dot{\theta} = B \sin(B^\top \theta). \tag{3}$$

where $B \in \mathbb{R}^{N\times M}$ is the incidence matrix associated to the graph topology $\mathcal{G}(\mathcal{V}, \mathcal{E})$ with number of nodes $|\mathcal{V}| = N$ and number of edges $|\mathcal{E}| = M$, while $\theta = [\theta_1, \theta_2, \ldots, \theta_N]^\top$. In the literature (see [10]), a common measure of the level of synchronisation for the system is given by the magnitude of Re^{ψ}, called *order parameter*. More precisely,

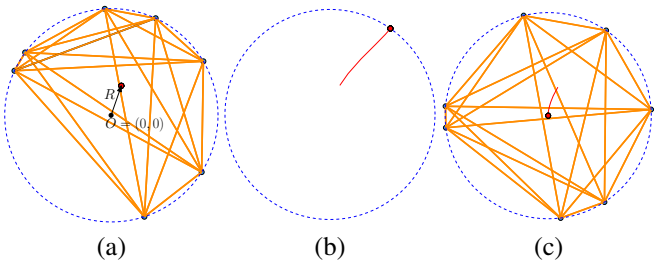

Fig. 1. Example of Kuramoto equilibria for $N = 7$ agents (blue circles) with a complete graph topology. The order parameter (4) is reported with a red circle and its time evolution with a thin red line. (a) Random initial configuration $\theta(0)$. (b) Equilibrium for the agents' synchronisation ($R = 1$) obtained with the classic Kuramoto dynamics. (c) Equilibrium for the balanced deployment ($R = 0$) obtained through (3) (dual behaviour).

$$R\, e^{\psi} = \frac{1}{N} \sum_{i=1}^{N} e^{j\,\theta_i}, \tag{4}$$

it represents in the complex plane the mean of the agents' positions. When $R = 1$ the system falls in the case of full synchronisation (or consensus, i.e. all the agents converge to a common state). On the other side, when $R = 0$, the agents in the system are in a balanced configuration. The order parameter, i.e. the modulus of (4), can be also written as a function of the graph topology:

$$r^2 = 1 - \frac{1}{N^2} \left([\cos\theta]^\top L [\cos\theta] + [\sin\theta]^\top L [\sin\theta] \right), \tag{5}$$

where $L = BB^\top$ is the Laplacian matrix associated to the graph topology, also equal to the difference between the degree matrix D and the adjacency matrix A, i.e., $L = D - A$. By selecting as Lyapunov candidate the function $V(\theta) = r^2$, we have

$$\dot{V}(\theta) = \nabla_\theta V \cdot \dot{\theta} = -\frac{2}{N^2} B \sin(B^\top\theta)\dot{\theta} = -\frac{2}{N^2} \dot{\theta}^\top \dot{\theta} \leq 0.$$

By the LaSalle invariance principle [22] the system will converge to an equilibrium, i.e., $\dot{\theta}(\infty) = 0_N$.

It is worthwhile to note that, for the complete graph topology, while for the classic Kuramoto dynamics the system goes towards the synchronisation of all the agents (i.e. $R \to 1$), by adopting (3), the system converges to a balanced deployment (i.e. $R \to 0$). To clarify this point, Figure 1-a depicts a random starting configuration with $N = 7$ agents (blue dots on the circle) and a complete graph topology (the edges of the graph are represented with orange lines connecting the agents). The red circle represents the order parameter position (4), assuming the centre of the circle as the origin $O = (0, 0)$. In Figure 1-b,c we depict the final configurations reached respectively by enforcing the classic Kuramoto dynamics (with positive coupling) and the time-inverted (i.e., with negative coupling) Kuramoto dynamics (3).

Given the Kuramoto system thus described, the main objective of the paper is to characterise the equilibrium configurations of (1) and their stability properties for specific graph topologies. We will also design controls to steer the agents between stable configurations. Notice that in the paper we use the terms "oscillator's phase" or "agent's position" with the same meaning, in the sense that the phase of an oscillator univocally identifies the position of an agent on the closed curve considered (i.e., the circle).

III. SYSTEM ANALYSIS

A. κ-clustered coverage

By considering the dynamics in (1) with the undirected circulant topology (2), by using basic trigonometry properties, it can be shown that θ is an equilibrium configuration if and only if

$$\text{diag}(\cos\theta)A\sin\theta = \text{diag}(\sin\theta)A\cos\theta. \tag{6}$$

Let us define $\theta^{\star(p)} = [\theta_1^{\star(p)}, \theta_2^{\star(p)}, \ldots, \theta_N^{\star(p)}]^\top$ the equilibrium point, whose configuration is circular symmetric (i.e., it is possible to assume $\theta_1^{\star(p)} = 0$). By exploiting the properties of circulant matrices [23], [24], it results

$$\theta^{\star(p)} = \left[0, \frac{2\pi p}{N}, \ldots, \frac{2\pi p(N-1)}{N}\right]^\top \tag{7}$$

(see [23] for the detailed derivation). To check the stability for the different values of $p \in \mathbb{N}$, we have to linearise the dynamics (1). The eigenvalues of the associated Jacobian matrix $J(p)$ can be computed analytically, since the matrix is also circulant (as reported in [23]).

Notice that, if we are considering generic undirected μ-circulant graphs, that indicates circulant topologies where the cardinality of the neighbour set $|\mathcal{N}_i| = \mu\ , \forall i$, there exist additional *exotic* stable equilibrium configurations [25] (as is shown in Figure 1-c, where we considered an $(N-1)$-circulant graph). Let us denote with f_i the phasor associated to agent i, and its neighbour set as $\mathcal{N}_i$. In [9], it is proved that an equilibrium satisfies the parallelism constraint between $\sum_{j\in\mathcal{N}_i} f_j$ and f_i, $\forall i$. For the case of 2-circulant topologies, i.e. with adjacency matrix (2) with $c_1 = 1$ and $c_k = 0, \forall\, k \neq 1$, the eigenvalues associated with the linearised system are given by

$$\lambda_r(J(p)) = -2\cos\left(\frac{2\pi p}{N}\right)\left[-1 + \cos\left(\frac{2\pi r}{N}\right)\right]. \tag{8}$$

Hence, the equilibrium (7) is stable if and only if $p \in (N/4, 3N/4)$, according to linear system theory [26]. When we restrict to 2-circulant graph topologies, all the stable equilibria are subsumed by the form (7). Indeed, due to the Jacobian matrix $J(p)$ structure, the stability condition is given by $\sum_{j\in\mathcal{N}_i}\cos(\theta_i - \theta_j) < 0$, $\forall i$, that, once combined with the phasors parallelism, returns the equilibrium configurations (7) with $p \in (N/4, 3N/4)$. However, we can be more flexible; let us define the ring topology, where each agent has $|\mathcal{N}_i| = 2$ and $|\mathcal{V}| = |\mathcal{E}| > 2$. By considering a ring topology these results hold true; since an equilibrium point for a 2-circulant topology is an equilibrium point also for a ring topology and the associated eigenvalues are necessarily the same. As a consequence, the rest of the paper will focus on the ring topologies equilibrium configurations (7). At this point, denoting the set of prime numbers as $\mathbb{N}^{\mathcal{P}}$, we are in the position to prove one of the main results of the paper:

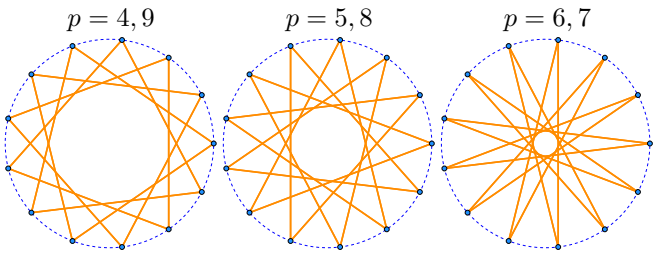

Fig. 2. Stable equilibrium configurations for $N = 13$, i.e. $p = [4, 5, 6, 7, 8, 9]$.

Lemma 1. *Given $N \in \mathbb{N}^{\mathcal{P}}$ and $p \in \mathbb{N}$ in the interval $0 < p < N$, the equilibrium positions $\theta^{\star(p)}$ in* (7) *splits the circle in N equal parts.*

Proof. The fact that N is a prime number and $p \in (0, N) \subset \mathbb{N}$ implies that $\theta^{\star(p)}$ positions on the circle (i.e., modulo 2π) and defined in (7) are all different. The fact that the circle is equally divided in N parts, follows from the difference between two consecutive positions, which remains constant and equals to $\Delta\theta_i^{\star(p)} = \theta_{i+1}^{\star(p)} - \theta_i^{\star(p)} = \frac{2\pi p}{N}$ for $p \in \mathbb{N}$ and $\forall i = 1, \ldots, N-1$. Moreover, $\Delta\theta_N^{\star(p)} = \theta_1^{\star(p)} - \theta_N^{\star(p)} = 0 - \frac{2\pi p(N-1)}{N} = \frac{2\pi p}{N} - 2\pi p$, which is equal to the others modulo 2π. □

Figure 2 graphically represents the different stable equilibrium configurations for $N = 13$ when the $p \in (N/4, 3N/4)$. According to what is stated in Lemma 1, all the possible final configurations make the agents reach the splay state formation over the circle. One interesting fact is that the set $N/4 < p < 3N/4$ can be split into two symmetric sets $\mathcal{P}' = (N/4, N/2)$ and $\mathcal{P}'' = (N/2, 3N/4)$. From Lemma 1, it follows immediately that the reached coverage configuration on the circle for $p' \in \mathcal{P}'$ is the same by permutation for a $p'' \in \mathcal{P}''$, i.e., being P a permutation matrix and selecting one value $p' \in \mathcal{P}'$, $\exists!\, p'' \in \mathcal{P}''$ such that $\overline{\theta}^{\star(p')} = P\theta^{\star(p')}$ and $\Delta\theta_i^{\star(p'')} = \Delta\overline{\theta}_i^{\star(p')}$. In particular, organising $\mathcal{P}'$ in ascending order, i.e. $p'_j < p'_{j+1}$, $\forall j$, and $\mathcal{P}''$ in descending order, i.e. $p''_j > p''_{j+1}$, $\forall j$, we have the same equilibrium for the pair $\{p'_j, p''_j\}$, $\forall j$. With reference to Figure 2, we have then that the same final coverage is reached for $p = \{4, 9\}$, $p = \{5, 8\}$ and for $p = \{6, 7\}$. Notice that these considerations about the solution symmetry are true in case of generic N and can be extended also for $p \in [0, N]$.

In light of Lemma 1, we can state what follows.

Theorem 1. *[The Solitude of prime numbers] Given $N \in \mathbb{N}^{\mathcal{P}}$ and the initial positions $\theta(0)$ are not in an unstable equilibrium point, by imposing* (3) *and considering a fixed ring topology, the overall system achieve a splay state pattern over the circle i.e., it achieves static coverage.*

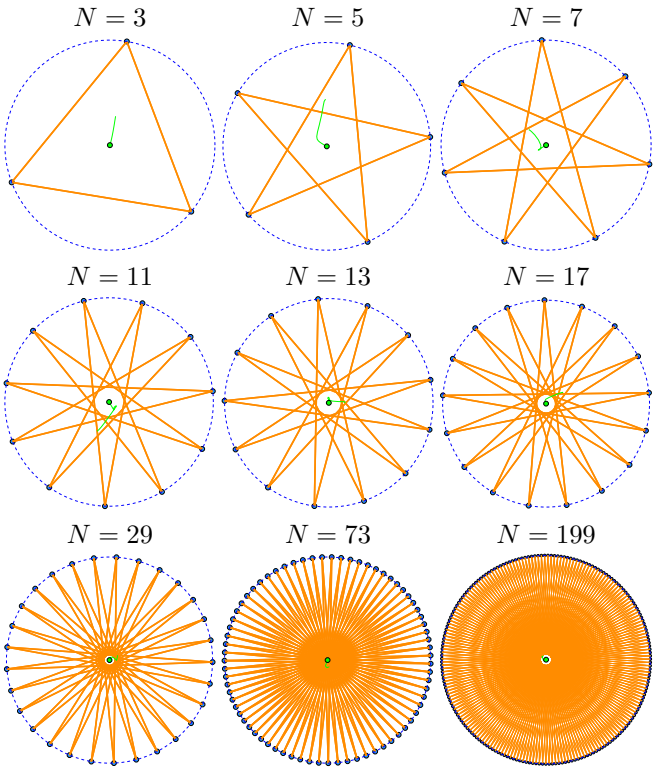

Fig. 3. Final equilibrium configurations obtained by imposing (3) with different number of agents $N \in \mathbb{N}^{\mathcal{P}}$ and starting from random initial positions $\theta(0)$. We depict in green the position of the global order parameter (4) to highlight the coverage reached configuration.

Proof. Since the system do not start from an unstable equilibrium configuration, it will converge to a stable equilibrium configuration by the LaSalle invariance principle. Since we assumed a time-invariant ring topology, the stable equilibrium configurations are characterised by (7) with $p \in (N/4, 3N/4)$. Since $N \in \mathbb{N}^{\mathcal{P}}$, the proof follows from Lemma 1. □

Figure 3 exemplifies the equilibrium configurations obtained from the evolution of the dynamics in (3) with fixed ring topology $\mathcal{R}$ and randomly generated starting positions $\theta(0)$. We picked different $N \in \mathbb{N}^{\mathcal{P}}$; the agents reach a splay state pattern on the circle, according to the Theorem 1.

Now we extend the results of Theorem 1 for generic $N \in \mathbb{N} \setminus \{0, 1\}$. To this end, we first have to distinguish between two different kind of stable equilibria, namely static coverage or static coverage in clusters, as reported in what follows.

Definition 1. *We define a* cluster *in the equilibrium configuration two positions $\theta_i^{\star(p)}$ and $\theta_j^{\star(p)}$ such that $\theta_i^{\star(p)} - \theta_j^{\star(p)} = 2a\pi$, with $a \in \mathbb{N}$.*

Lemma 2. *Given $N \in \mathbb{N} \setminus \{0, 1\}$, the number of agents that clusters together at the equilibrium is given by the maximum common divider between N and p, denoted by $\kappa = mcd(N, p)$. The agents' clusters subdivide the circle in N/κ equal parts.*

Proof. By considering the stable equilibrium in (7), dividing both numerator and denominator by κ, we can rewrite

$$\theta^{\star(p)} = \left[0, \frac{2\pi p/\kappa}{N/\kappa}, \ldots, \frac{2\pi p/\kappa (N-1)}{N/\kappa}\right]^{\top}. \tag{9}$$

It can be noticed that when $p = \kappa$, the equilibrium (9) imposes a circle subdivision in N/κ equal parts, hence κ is the number of agents clustered together. When $p \neq \kappa$ and $\kappa \geq 1$, since $p/\kappa \in \mathbb{N} \setminus \{0, 1\}$ the circle is still divided in N/κ parts with κ clustered agents. □

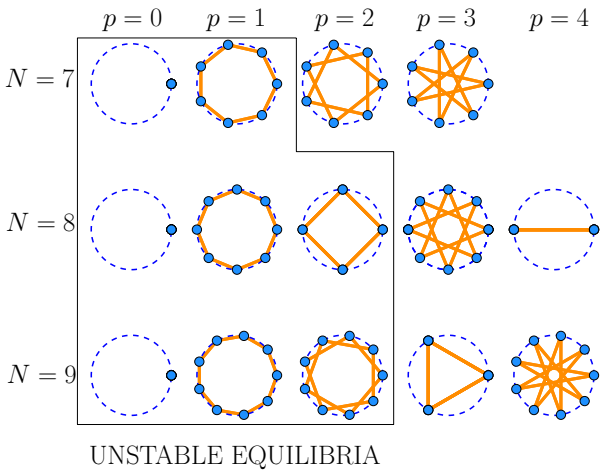

Fig. 4. Stable and unstable equilibrium configurations (7) for the dynamics (3) with fixed 2-circulant topologies. We show the different equilibrium configurations by varying the values of p and the number of agents, which are $7, 8, 9$ respectively.

We call the equilibrium configuration described by Lemma 2 as κ-clustered coverage. With this terminology, we can then denote the synchronisation case as an N-clustered coverage, while the splay state pattern is equivalent to 1-clustered coverage. All the possible κ-clustered coverage equilibria, either stable and unstable, for $N = \{7, 8, 9\}$ agents, are depicted in Figure 4. First, notice that regardless of the number of agents and by means of (9), we have N-clustered coverage (i.e., agents synchronisation) for $p = 0$, which is for the dynamics (3) an unstable equilibrium configuration in light of (8) (which will be adopted in the following to characterise the unstable configurations). Similarly, for $p = 1$ we have unstable equilibria, all related to a 1-clustered coverage (maximum coverage) for Lemma 2. On the top row of Figure 4, we have the case of $N = 7$ always reaching 1-clustered coverage (under the assumption that $0 < p < N$) since N is prime and in light of Lemma 2. While for $p = \{0, 7\}$ the system is in a 7-clustered coverage. The middle raw reports the case of $N = 8$, always exhibiting a κ-clustered coverage: using Lemma 2, it follows that for $p = \{1, 3, 5, 7\}$ we have a 1-clustered coverage; for $p = 2$ or $p = 6$ a 2-clustered coverage; for $p = 4$ we have instead a 4-clustered coverage, while for $p = \{0, 8\}$ the system is in an 8-clustered coverage (i.e. synchronisation case). Notice that the equilibrium for $p = \{0, 1, 2, 6, 7, 8\}$ are unstable. Finally, the bottom row considers $N = 9$, it reaches 9-clustered

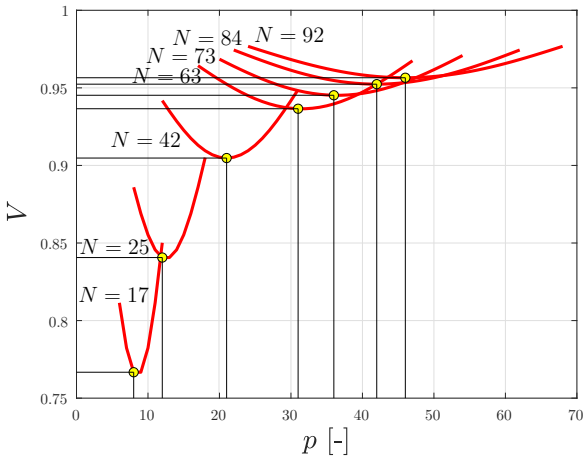

Fig. 5. The potential values $V = r^2$ as a function of p and the number of agents N. The yellow circles indicate the minimum values of the potential, which always correspond to $p = \lfloor N/2 \rfloor$.

coverage for $p = \{0, 9\}$, unstable 1-clustered coverage for $p = \{1, 2, 7, 8\}$, a stable 3-clustered coverage when $p = 3$ and $p = 6$, a stable 1-clustered coverage for $p = \{4, 5\}$.

Definition 2. *We define the stability degree of an equilibrium the value attained by the Lyapunov function $V(\theta) = r^2$.*

To identify the equilibrium with lowest Lyapunov function value (with a slight language abuse named *most stable equilibrium*), the following Lemma turns useful.

Lemma 3. *Given the dynamics in* (3)*, the most stable equilibrium corresponds to the one maximising the difference $\Delta\theta^{\star(p)}$ between linked agents, it matches with $p = \lfloor N/2 \rfloor$ in* (7)*.*

Proof. As is reported in [10], the order parameter, in (5) for the case of ring topologies, can be rewritten as

$$r^2 = \frac{N^2 - 2N + 1_N^\top \cos(B^\top \theta)}{N^2}, \tag{10}$$

hence the Lyapunov function $V = r^2$ is minimised when the positions' differences $\phi = B^\top \theta$ are equal to π. As a consequence, the most stable configuration is the one that maximises the distance between linked agents. By considering the equilibrium in (7), it is reached when $p = N/2$ if N is even (i.e., $\Delta\theta^{\star(N/2)} = \pi$), and for $p = (N \pm 1)/2$ if N is an odd number ($\Delta\theta^{\star((N\pm1)/2)} = \pi - \pi/N$), which is a splay state pattern. Hence, the proof. □

In Figure 5, we depict the value that assumes $V = r^2$ as a function of $p \in (N/4, 3N/4)$ for different N. For each curve, according to Lemma 3, the global minimum of the potential function is reached at $p = \lfloor N/2 \rfloor$.

IV. TOWARDS THE CONTROL OF THE FINAL EQUILIBRIUM CONFIGURATION

Computing a-priori the final equilibrium configuration, given the initial conditions, is a challenging problem, however some insights can still be derived. Using the concept of stability degree given in Definition 2 and assuming that $\mathcal{C}$ is the set of controllable agents, i.e., the agents whose position can be controlled, we found that it is always possible to change the equilibrium configuration of the overall system by acting on the position $\theta_{\mathcal{C}}$, as stated in the following conjecture.

Conjecture 2. *Given $N \in \mathbb{N} \setminus \{0, 1\}$ with a fixed ring topology, if the agents' position are in a stable configuration with a certain value of $p \neq \lfloor N/2 \rfloor$ and the position of a single agent $i \in \mathcal{C}$ is changed from θ_i to $\theta_i + \Delta\theta_i$, the time evolution of the system* (3) *surely reaches a final equilibrium configuration corresponding to $p^+ = p \pm 1$ such that $|p^+ - \lfloor N/2 \rfloor| < |p - \lfloor N/2 \rfloor|$ if $\Delta\theta_i = \pi$. If $p = \lfloor N/2 \rfloor$, the change of the position does not change the equilibrium configuration.*

Notice that, if the aim of an agent $i \in \mathcal{C}$ is to steer the system in a splay configuration, this is always possible when the number of agents N is odd. In fact, the most stable equilibrium configuration in the sense of Lemma 3 is always in a splay configuration (i.e., 1-clustered coverage). In the case of an even N, it results that the most stable equilibrium configuration is an $N/2$-cluster coverage, i.e. all the agents are clustered at two opposite positions. Conjecture 2 ensures that the unique controlled agent $i \in \mathcal{C}$ can always steer the system to reach that configuration. However, one single agent cannot switch the system to a less stable configuration: to this end, we need the following additional conjecture.

Conjecture 3. *Given an even number of agents N with a fixed ring topology, if the agents' positions are in a stable configuration with a certain value of $p = N/2$ and the positions of the agents $i, j \in \mathcal{C}$, with $j \in \mathcal{N}_i$, are changed from θ_i to $\theta_i + \Delta\theta_i$ and θ_j to $\theta_j + \Delta\theta_j$, the time evolution of the system* (3) *reaches a final equilibrium configuration corresponding to $p^+ = p \pm 1$ such that $V(\theta^{\star p^+}) > V(\theta^{\star p})$. The configuration $p^+ = N/2 \pm 1$ is a splay configuration only if $N/2$ is an even number .*

We can then state that if the cardinality $|\mathcal{C}| = 1$, it is possible only to move along more stable configurations, while if $|\mathcal{C}| = 2$ both switches are feasible. These results are not formally proved in this version of the paper, however we validated them through extensive simulations. Figure 6 reports an example for $N = 24$ in which the value of the Lyapunov function is plotted as a function of the controlled position shift $\Delta\theta_i$. By perturbing the agent $i \in \mathcal{C}$ of an amount equal to $\Delta\theta_i$, the value $V(\theta)$ can only decrease, hence reaching more stable configurations according to Definition 2. Moreover, the value of p is always decreased of at most 1, unless the minimum configuration is considered, i.e. the one with $p = \lfloor N/2 \rfloor$, where no switch can be observed, according to Conjecture 2. Another important information is related to the value of $\Delta\theta_i$ that is necessary to fire the switch: as the configuration is more stable (i.e. with increasing p), the smaller is the set of controlled actions $\Delta\theta_i$ to apply on the i–th agent. Nonetheless, $\Delta\theta_i = \pi$ is alway able to apply a configuration switch (see Conjecture 2).

To show empirical validity of Conjecture 3, we show in Figure 7 the controlled positions feasible pairs $\Delta\theta_i$ and

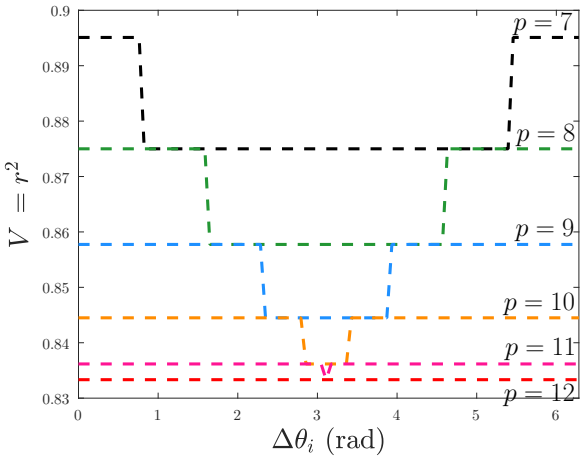

Fig. 6. Starting from the equilibrium configuration p, by selecting $\mathcal{C} = \{i\}$, we depict the potential values $V = r^2$ as a function of $\Delta\theta_i$. The system has $N = 24$ agents.

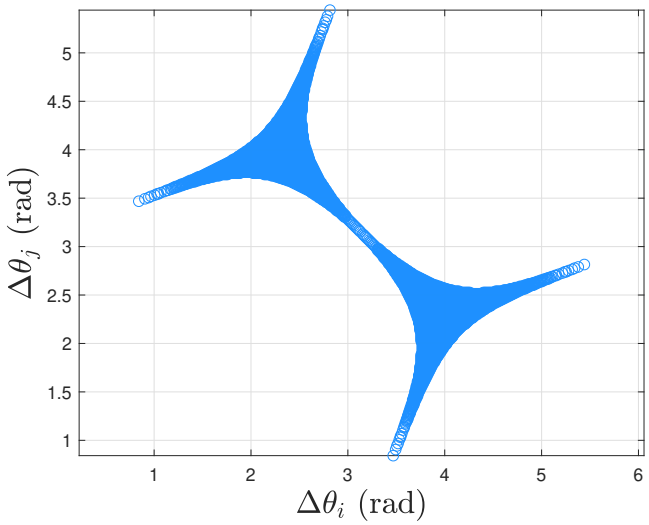

Fig. 7. Set of position differences $\Delta\theta_i$ and $\Delta\theta_j$ for the i–th and j–th agents which enables an equilibrium switch from $p = N/2$ towards $p = N/2 - 1$.

$\Delta\theta_j$ to enforce the equilibrium configuration switch from $p = N/2$ to $p = N/2 - 1$. The map in Figure 7 is generic i.e. it is valid for any choice of N.

Finally, Figure 8 shows the time evolution of the Lyapunov function $V(\theta)$ and the reached stable configurations for a network of $N = 20$ agents. We started from a random configuration and the system evolves towards the stable configuration with $p = 6$. From the stable configuration with $p = 6$, we control the first agent position, which is $\theta_1^{\star(p)} = 0$, towards $\theta_1^{\star(p)} = \pi$, thus switching to another stable configuration with $p = 7$, reached after 2 seconds. The position change is performed three more times every 2 seconds, thus leading first to $p = 8$, $p = 9$ and then to $p = 10$, which is the most stable configuration according to Lemma 3. At this time, by perturbing the positions of two agents, picking the position differences from the map

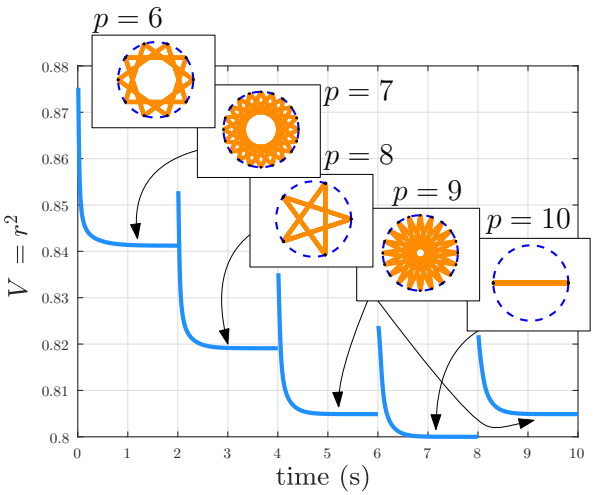

Fig. 8. Time evolution of $V(\theta) = r^2$ for a network with $N = 20$ agents. For $t = 0$ s and every 2 seconds, we select one single agent and we apply a controlled position shift $\Delta\theta = \pi$. As a result, the system switches towards more stable configurations, until the minimum value for $p = 10$ is reached at $t = 8$ s. At this time, the set of controllable agents is enlarged, i.e. $|\mathcal{C}| = 2$ and, by applying the differences of positions reported in Figure 7, the final system configuration is brought back to $p = 9$.

in Figure 7, the system returns to the configuration $p = N/2 - 1 = 9$, which is a splay state pattern since $N/2$ is an even number.

V. CONCLUSIONS

We analysed the time inverted Kuramoto model with a fixed ring graph topology. We discussed the equilibrium configurations of the dynamical system, and we provide sufficient condition to achieve 1-clustered coverage. The cases where κ-clustered coverage occurs is discussed and we propose two conjectures to study the controllability of the equilibria. In the near future, we plan to study more deeply the controllability of the equilibria, considering time-varying communication topologies, communication delays and generic graph topologies e.g. directed graphs. We are also interested in studying how to increase the system resiliency against generic cyber-attacks using the results from the controllability analysis. Another interesting research direction is related to persistent monitoring algorithms on generic closed curves; it can be analysed both the case of homogeneous persistent monitoring and the case where there are points of interest that require higher monitoring frequencies.

REFERENCES

[1] T. Vicsek, "A question of scale," *Nature*, vol. 411, no. 6836, pp. 421–421, 2001.

[2] M. Boldrer, L. Palopoli, and D. Fontanelli, "A unified lloyd-based framework for multi-agent collective behaviours," *Robotics and Autonomous Systems*, submitted.

[3] J. A. Acebrón, L. L. Bonilla, C. J. P. Vicente, F. Ritort, and R. Spigler, "The kuramoto model: A simple paradigm for synchronization phenomena," *Reviews of modern physics*, vol. 77, no. 1, p. 137, 2005.

In `https://www.youtube.com/watch?v=AQxW9aP8ugo` we provide a video with the results of a simulation similar to that shown in Figure 8.

[4] F. Dörfler and F. Bullo, "Synchronization in complex networks of phase oscillators: A survey," *Automatica*, vol. 50, no. 6, pp. 1539–1564, 2014.
[5] E. Brown, P. Holmes, and J. Moehlis, "Globally coupled oscillator networks," in *Perspectives and Problems in Nolinear Science*. Springer, 2003, pp. 183–215.
[6] D. A. Paley, N. E. Leonard, R. Sepulchre, D. Grunbaum, and J. K. Parrish, "Oscillator models and collective motion," *IEEE Control Systems Magazine*, vol. 27, no. 4, pp. 89–105, 2007.
[7] A. T. Winfree, "Biological rhythms and the behavior of populations of coupled oscillators," *Journal of theoretical biology*, vol. 16, no. 1, pp. 15–42, 1967.
[8] Y. Kuramoto, "Self-entrainment of a population of coupled non-linear oscillators," in *International symposium on mathematical problems in theoretical physics*. Springer, 1975, pp. 420–422.
[9] P. Monzón and F. Paganini, "Global considerations on the kuramoto model of sinusoidally coupled oscillators," in *Proceedings of the 44th IEEE Conference on Decision and Control*. IEEE, 2005, pp. 3923–3928.
[10] A. Jadbabaie, N. Motee, and M. Barahona, "On the stability of the kuramoto model of coupled nonlinear oscillators," in *Proceedings of the 2004 American Control Conference*, vol. 5. IEEE, 2004, pp. 4296–4301.
[11] R. Bertollo, E. Panteley, R. Postoyan, and L. Zaccarian, "Uniform global asymptotic synchronization of kuramoto oscillators via hybrid coupling," in *21st IFAC World Congress, IFAC 2020*, 2020.
[12] T. Menara, G. Baggio, D. S. Bassett, and F. Pasqualetti, "Stability conditions for cluster synchronization in networks of heterogeneous kuramoto oscillators," *IEEE Transactions on Control of Network Systems*, vol. 7, no. 1, pp. 302–314, 2019.
[13] R. Sepulchre, D. A. Paley, and N. E. Leonard, "Stabilization of planar collective motion: All-to-all communication," *IEEE Transactions on Automatic Control*, vol. 52, no. 5, pp. 811–824, 2007.
[14] ——, "Stabilization of planar collective motion with limited communication," *IEEE Transactions on Automatic Control*, vol. 53, no. 3, pp. 706–719, 2008.
[15] Z. Xu, M. Egerstedt, G. Droge, and K. Schilling, "Balanced deployment of multiple robots using a modified kuramoto model," in *2013 American Control Conference*. IEEE, 2013, pp. 6138–6144.
[16] H. Hong and S. H. Strogatz, "Kuramoto model of coupled oscillators with positive and negative coupling parameters: an example of conformist and contrarian oscillators," *Physical Review Letters*, vol. 106, no. 5, p. 054102, 2011.
[17] M. Sinha, F. Dörfler, B. Johnson, and S. Dhople, "Phase balancing in globally connected networks of liénard oscillators," in *2017 IEEE 56th Annual Conference on Decision and Control (CDC)*. IEEE, 2017, pp. 595–600.
[18] F. Ferrante and Y. Wang, "Robust almost global splay state stabilization of pulse coupled oscillators," *IEEE Transactions on Automatic Control*, vol. 62, no. 6, pp. 3083–3090, 2017.
[19] S. Phillips and R. G. Sanfelice, "Robust asymptotic stability of desynchronization in impulse-coupled oscillators," *IEEE Transactions on Control of Network Systems*, vol. 3, no. 2, pp. 127–136, 2015.
[20] J. A. Marshall, M. E. Broucke, and B. A. Francis, "Formations of vehicles in cyclic pursuit," *IEEE Transactions on automatic control*, vol. 49, no. 11, pp. 1963–1974, 2004.
[21] P. J. Davis, *Circulant matrices*. American Mathematical Soc., 2013.
[22] J. P. La Salle, *The stability of dynamical systems*. SIAM, 1976.
[23] A. Townsend, M. Stillman, and S. H. Strogatz, "Dense networks that do not synchronize and sparse ones that do," *Chaos: An Interdisciplinary Journal of Nonlinear Science*, vol. 30, no. 8, p. 083142, 2020.
[24] G. H. Golub and C. F. Van Loan, *Matrix computations*. JHU press, 2013, vol. 3.
[25] E. A. Canale and P. Monzón, "Exotic equilibria of harary graphs and a new minimum degree lower bound for synchronization," *Chaos: An Interdisciplinary Journal of Nonlinear Science*, vol. 25, no. 2, p. 023106, 2015.
[26] J. P. Hespanha, *Linear systems theory*. Princeton university press, 2018.